Effect of Water Hydrogen Bonding on the Solvent-Mediated "Oscillatory" Repulsion of C 60 Fullerenes in Water

ARTICLE *in* JOURNAL OF PHYSICAL CHEMISTRY LETTERS · APRIL 2015

Impact Factor: 7.46 · DOI: 10.1021/acs.jpclett.5b00508

2 AUTHORS, INCLUDING:

Yuri S Djikaev
University at Buffalo, The State University of N…

70 PUBLICATIONS **834** CITATIONS

SEE PROFILE

THE JOURNAL OF PHYSICAL CHEMISTRY Letters

Letter

pubs.acs.org/JPCL

Effect of Water Hydrogen Bonding on the Solvent-Mediated "Oscillatory" Repulsion of C_{60} Fullerenes in Water

Yuri S. Djikaev* and Eli Ruckenstein*

Department of Chemical and Biological Engineering, SUNY at Buffalo, Buffalo, New York 14260, United States

ABSTRACT: The solvent-mediated interaction of C_{60} fullerenes in liquid water is examined by using the combination of the probabilistic hydrogen bond model with the density functional theory. This combination allows one to take into account the effect of hydrogen bonding between water molecules on their interaction with fullerenes and to construct an approximation for the distribution of water molecules in the system, which provides an efficient foundation for studying hydrophobic phenomena. Our numerical evaluations predict the solvent-induced interaction of two C_{60} fullerenes in water at 293 K to have an oscillatory-repulsive character (previously observed in molecular dynamics simulations) only when the vicinal water−water hydrogen bonds are slightly weaker than bulk ones. Besides indicating the direction of the energetic alteration of water−water hydrogen bonds near C_{60} fullerenes, our model also suggests that the hydrogen bonding ability of water plays a defining role in the solvent-mediated C_{60}−C_{60} repulsion.

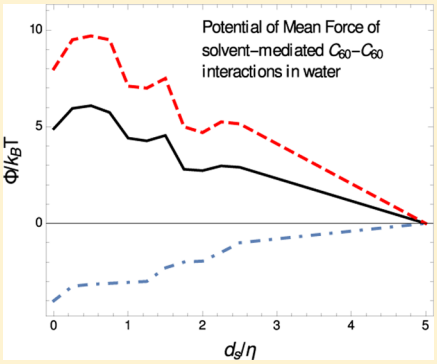

Fullerenes are a relatively recently discovered class of molecules composed entirely of carbon, in the form of a hollow sphere, ellipsoid, or tube.[1−3] The most remarkable of them is the C_{60} variant, also referred to as buckminsterfullerene.[1,4−6] Owing to their unique chemical and physical properties, C_{60} fullerenes have become the object of significant interest in many fields of biology and chemistry including polymer science, nanotechnology, and pharmaceuticals. For example, it was reported[7] that C_{60} fullerenes can bind to the HIV protease with high affinity, acting as an HIV virus inhibitor. The possibility of using buckminsterfullerene for cancer treatment is also currently being investigated; it has been shown to be cytotoxic, cleaving DNA when it is exposed to visible light.[8]

Many of the potential applications of C_{60} fullerenes, as well as their potential environmental and health effects, require the understanding of how C_{60} fullerenes and their derivatives solvate and self-associate in aqueous environments. The association behavior of C_{60} fullerenes in aqueous solution does not follow the conventional wisdom about hydrophobic phenomena. Indeed, C_{60} fullerenes are highly hydrophobic, virtually insoluble in water. However, as shown by molecular dynamics (MD) simulations,[4,5] the solvent-induced interactions of C_{60} fullerenes in aqueous solution has a repulsive character, in contrast to the attractive one observed for conventional hydrophobes. As a result, water was found to reduce the strong C_{60}−C_{60} attraction[4,5] thus weakening the C_{60}−C_{60} association, as opposed to enhancing the association of conventional hydrophobic particles.[9−12]

For the overall association interaction between two fullerenes, various explanations were proposed.[13,14] On the basis of MD simulations[4,5] it was suggested to be dominated by the van der Waals attraction, due to a very high density of C_{60} surface atoms; this also gives rise to strong C_{60}−water attraction, and hence a significant increase in water density oscillations near the fullerene. By means of the van Oss theory of the Lewis acid−base component of surface energy, it was found[13] that the overall interfacial attraction due to acid−base forces is responsible for the aggregation of C_{60} fullerenes.

In this paper, we attempt to shed some more light on the peculiar behavior of solvent-mediated interaction of two C_{60} fullerenes in liquid water by using our previously developed[15−19] combination of the probabilistic hydrogen bond (PHB) model with the density functional theory (DFT). Such a combination allows one to explicitly incorporate the effect of water−water hydrogen bonding on water−hydrophobe interactions into DFT and to construct an approximation for the distribution of water molecules in the system, which provides a reasonably good (much faster and accurate enough) alternative to the standard iteration procedure of DFT. The main points of the PHB model and its implementation into DFT are provided below (see refs15−19 for more details).

Consider two hydrophobic particles, 1 and 2, shaped as spherical shells (hollow spheres) of outer radii R_1 and R_2 and shell thickness δ_1 and δ_2, immersed in liquid water. Such a shape of particles roughly mimics the distribution of carbon atoms in globular fullerenes, including C_{60}.

Even if the intrinsic hydrogen bonding ability of a water molecule is not affected by a hydrophobe, in its vicinity a "vicinal" water molecule forms a smaller number of bonds than in bulk because the surface restricts the configurational space available to other water molecules necessary for a vicinal water molecule to form hydrogen bonds ("missing neighbor effect").

Received: March 10, 2015
Accepted: April 14, 2015
Published: April 21, 2015

DOI: 10.1021/acs.jpclett.5b00508
J. Phys. Chem. Lett. 2015, 6, 1761−1766

The probabilistic model allows one to obtain an analytic expression for the average number of bonds n_s that a vicinal water molecule (in the vicinity of a spherical hydrophobe) can form as a function of its distance to the hydrophobe and hydrophobe radius.[18] When the water molecule is close enough to two hydrophobes, n_s will depend on the distance between water molecule and each hydrophobe, the distance between two hydrophobes, and the radii of both hydrophobes. The distance d between the two spherical hydrophobes is the distance between their centers; the distance from the center of a water molecule S to the center of hydrophobe i of radius R_i (i = 1,2) is denoted by r_i. Thus, $n_s = n_s(R_1,R_2,d,r_1,r_2)$.

In the PHB model, the function $n_s = n_s(R_1,R_2,d,r_1,r_2)$ is represented as[19]

$$n_s = k_1 b_1 + k_2 b_1^2 + k_3 b_1^3 + k_4 b_1^4 \tag{1}$$

where b_1 is the probability that one of the hb-arms (of a bulk water molecule) can form a hydrogen bond; the coefficients k_1, k_2, k_3, and k_4 as functions of R_1, R_2, d, r_1, and r_2 can be found via geometric considerations.[19] They all become equal to 1 if both $r_1 \geq R_1 + 2\eta$ and $r_2 \geq R_2 + 2\eta$, when eq 1 reduces to $n_b = b_1 + b_1^2 + b_1^3 + b_1^4$, with n_b being the number of hydrogen bonds per bulk water molecule.[15]

Consider a layer of thickness η from $r_i = R_i + \eta$(minimal distance between water molecule and hydrophobe i) to $r_i = R_i + 2\eta$ around hydrophobe i (i = 1,2) and denote it by SHL_i ("solute hydration layer i"). Denote the energy of a bulk (water−water) hydrogen bond by $\varepsilon_b < 0$ and the energy of a vicinal hydrogen bond by $\varepsilon_s < 0$. The PHB model imposes no restriction on the latter, so it is valid independent of whether $\varepsilon_b < \varepsilon_s$ or $\varepsilon_b = \varepsilon_s$, or $\varepsilon_b > \varepsilon_s$.

The deviation of n_s from n_b and the deviation of ε_s from ε_b give rise to a hydrogen bond contribution to the external potential field whereto a water molecule is subjected in the vicinity of two hydrophobes. This contribution, U_{ext}^{hb}, can be determined as[19]

$$U_{ext}^{hb} \equiv U_{ext}^{hb}(R_1, R_2, d, r_1, r_2) = \frac{1}{2}(\varepsilon_s n_s - \varepsilon_b n_b) \tag{2}$$

where the first term on the RHS represents the total energy of hydrogen bonds of the water molecule near the hydrophobes, whereas the second term is the energy of its hydrogen bonds in bulk.

Due to its complexity, the effect of a hydrophobic surface on the hydrogen bonding ability of water molecules had been until recently ignored in DFT. Using the PHB model, this problem can be solved[16−19] by representing the overall external potential $U_{ext} \equiv U_{ext}(R_1,R_2,d,r_1,r_2)$, whereto a water molecule is subjected in the vicinity of two spherical hydrophobes, as

$$U_{ext} = U_{ext}^{pw} + U_{ext}^{hb} \tag{3}$$

where $U_{ext}^{pw} \equiv U_{ext}^{pw}(R_1,R_2,d,r_1,r_2)$ represents the pairwise interactions of a fluid molecule with the molecules of the substrate and the effect of the latter on the interactions between fluid molecules themselves.[20]

The solvent-mediated interaction of solute particles can be characterized by the potential of mean force,[21] $\Phi \equiv \Phi(R_1,R_2,d)$, which depends on the radii of both solutes as well as on the distance d between them. In an open system (a grand canonical ensemble of constant chemical potential μ, volume V, and temperature T), one can write that $\Phi = \Omega - \Omega_\infty$, where Ω is the grand thermodynamic potential of the system with the two solutes at distance d and $\Omega_\infty \equiv \Omega|_{d=\infty}$.

In DFT, the grand thermodynamic potential Ω of a single component fluid, subjected to an external potential U_{ext}, is a functional[20] of the number density $\rho(\mathbf{r})$ of fluid molecules

$$\Omega[\rho(\mathbf{r})] = \mathcal{F}_h[\rho(\mathbf{r})] + \frac{1}{2}\iint d\mathbf{r}\, d\mathbf{r}'\rho(\mathbf{r})\rho(\mathbf{r}') \times \phi_{at}(|\mathbf{r}-\mathbf{r}'|) + \int d\mathbf{r} U_{ext}(R,\mathbf{r})\rho(\mathbf{r}) - \mu\int d\mathbf{r}\rho(\mathbf{r}), \tag{4}$$

where $\mathcal{F}_h[\rho(\mathbf{r})]$ is the intrinsic Helmholtz free energy functional of hard sphere fluid, μ is the chemical potential, and $\phi_{at}(|\mathbf{r}-\mathbf{r}'|)$ is the attractive part of the interaction potential between two fluid molecules located at $\mathbf{r}$ and $\mathbf{r}'$; the integrals are taken over the volume V of the system. For $\mathcal{F}_h[\rho(\mathbf{r})]$, the weighted density approximation (WDA)[22,23] with a weight function independent of weighted density $\tilde{\rho}(\mathbf{r})$ represents an optimal combination of accuracy and simplicity.

The equilibrium density profile is obtained by minimizing $\Omega[\rho(\mathbf{r})]$ with respect to $\rho(\mathbf{r})$. The corresponding Euler−Lagrange equation can be written as

$$\mu = k_B T \ln(\Lambda^3\rho(\mathbf{r})) + W(\mathbf{r};\rho(\mathbf{r})) \tag{5}$$

where $\Lambda = (h^2/2\pi m k_B T)^{1/2}$ is the thermal de Broglie wavelength of a molecule of mass m (h and k_B being Planck's and Boltzmann's constants), and $W(\mathbf{r};\rho(\mathbf{r}))$ is a function of $\mathbf{r}$ and a functional of $\rho(\mathbf{r})$ (see refs 17−20, 22, and 23, for more details), involving $\phi_{at}(|\mathbf{r}-\mathbf{r}'|)$ and $\Delta\psi_h(\rho)$, the configurational part of the free energy of hard sphere fluid per molecule, as well as its derivative $\Delta\psi_h'(\rho) \equiv d\Delta\psi_h(\rho)/d\rho$.

If the hydrophobes are spherical particles, the density distribution of fluid molecules exhibits the axial symmetry with respect to the line passing through the centers of both hydrophobes. One can choose that line as the axis z of a cylindrical coordinate system q,ϕ,z, with the origin in the center of hydrophobe 1 and positive direction of axis z from hydrophobe 1 to hydrophobe 2, q the distance from the axis z, and ϕ the polar angle (in the plane perpendicular to the axis z). The equilibrium density profile obtained from eq 5 is then a function of two variables, q and z, i.e., $\rho(\mathbf{r}) = \rho(q,z)$. The substitution of $\rho(q,z)$ into eq 4 provides the grand thermodynamic potential Ω of the system.

For a numerical illustration, we considered two identical hydrophobic spherical shells of outer radius $R \equiv R_1 = R_2 = 2\eta$ nm and shell thickness $\delta \equiv \delta_1 = \delta_2$, inserted in the model water at temperature T = 293.15 K and chemical potential $\mu = -11.5989\, k_B T$ corresponding to its two-phase equilibrium. The liquid state of bulk water was ensured by imposing the appropriate boundary condition onto eq 5, $\rho(r) \to \rho_l$ as $r \to \infty$, with $r = \sqrt{q^2 + z^2}$ and ρ_l the bulk liquid density. The densities ρ_v and ρ_l of coexisting vapor and liquid, respectively, are determined by solving the equations $\mu(\rho,T)|_{\rho=\rho_v} = \mu(\rho,T)|_{\rho=\rho_l}$ and $p(\rho,T)|_{\rho=\rho_v} = p(\rho,T)|_{\rho=\rho_l}$, requiring the chemical potential $\mu \equiv \mu(\rho,T)$ and pressure $p \equiv p(\rho,T)$ to be the same throughout both coexisting phases.

The chemical potential of a uniform hard sphere fluid μ_h and $\Delta\psi_h$ were modeled in the Carnahan−Starling approximation.[24] The weight function $w(|\mathbf{r}' - \mathbf{r}|;\tilde{\rho}(\mathbf{r}))$ was adopted to be

DOI: 10.1021/acs.jpclett.5b00508
J. Phys. Chem. Lett. 2015, 6, 1761−1766

$\tilde{\rho}$-independent,[22] $w(r_{12}) = \Theta(\eta - r_{12})3(\eta - r_{12})/(\pi\eta^4)$, with $\Theta(u)$ being the Heaviside (unit-step) function.

The pairwise interactions of water molecules were modeled by using the Lennard-Jones (LJ) potential with the energy parameter $\varepsilon_{ww} = 5.4 \times 10^{-14}$ erg and the diameter d of a model molecule set to equal the length η of a hydrogen bond. The attractive part ϕ_{at} of pairwise water−water interactions was modeled via the Weeks−Chandler−Anderson perturbation scheme.[25] The interaction between the water molecule and the carbon atom of C_{60} was assumed[4,5] to be of LJ type, with the energy parameter $\varepsilon_{wc} \simeq 0.603\varepsilon_{ww}$ (in most of the calculations) and a length parameter η. The carbon atoms of C_{60} were *assumed* to be uniformly distributed with the dimensionless density $\rho_p\eta^3 \approx 1.75$ in a spherical shell of thickness $\delta = \eta$. Due to uncertainties concerning the parameters δ, ρ_p, and $k_{LJ} \equiv \varepsilon_{wc}/\varepsilon_{ww}$, some of the calculations were also carried out for different values of the latter, whereof the variation can indirectly take account of the uncertainties in δ and/or ρ_p.

For a qualitative illustration, time-consuming iterations, needed to solve eq 5, can be avoided. One can approximate the density profile $\rho(q,z)$ in the vicinity two spherical hydrophobes of *equal* radii by using a spherically symmetric density profile $\rho^{(1)}(r)$ in the vicinity of a single hydrophobe.

In the solute hydration layer of a *single* fullerene, the water density $\rho^{(1)}$ and number $n_s^{(1)}$ of hydrogen bonds per water molecule are well-defined, single-value functions of distance r, i.e., $\rho^{(1)} = \rho^{(1)}(r)$ and $n_s^{(1)} = n_s^{(1)}(r)$. Thus, one can introduce a function $\rho_{n_s}^{(1)}(n_s^{(1)})$ that defines a one-to-one relationship between $\rho^{(1)}$ and $n_s^{(1)}$ in the SHL of a single fullerene.

Divide the system into two halves by the plane $z = (1/2)d$ perpendicular to the z-axis in the middle between two fullerenes (now $R_1 = R_2 = R$). The density profile $\rho(q,z)$ can be approximated as

$$\rho(q,z) = \begin{cases} \rho^{(1)}(r_1) & (z \le d/2 \cap r_2 \ge R + 2\eta), \\ \rho^{(1)}(r_2) & (z > d/2 \cap r_1 \ge R + 2\eta), \\ \rho_{n_s}^{(1)}(n_s^{(1)}(R+\eta)) & (n_s(R,R,d,r_1(q,z),r_2(q,z)) \le n_s^{(1)}(R+\eta)), \\ \rho_{n_s}^{(1)}(n_s(R,R,d,r_1(q,z),r_2(q,z))) & (n_s(R,R,d,r_1(q,z),r_2(q,z)) > n_s^{(1)}(R_e+\eta)), \end{cases} \quad (6)$$

where r_i $(i = 1,2)$ is the distance from a given point (with coordinates q,z, and arbitrary ϕ) to the center of fullerene i: $r_1 = \sqrt{q^2 + z^2}$, $r_2 = \sqrt{q^2 + (z-d)^2}$.

In this approximation, in the overlap region of SHL_1 and SHL_2, the water density is determined by the number of H-bonds per water molecule, $n_s(R,R,d,r_1(q,z),r_2(q,z))$, and hence is conditioned by both hydrophobes. Outside the SHL_1/SHL_2 overlap region, the density of fluid molecules is determined by only one of the hydrophobes (either 1 or 2). The larger the value of d, the more accurate approximation 6. For a given separation $d_s \equiv d - (R + R + \eta)$, its accuracy decreases with increasing R due to the widening[16−19] of the transition layer "vapor at hydrophobe−liquid in bulk". For small hydrophobes, such as C_{60} fullerenes, this approximation can be expected to be acceptable.

The functions $\rho^{(1)} = \rho^{(1)}(r)$, used in eq 6, are presented as $\rho^{(1)}\eta^3$ versus r/η (with $r = 0$ corresponding to the center of the fullerene) in Figures 1 and 2. As the energetic alteration of a vicinal hydrogen bond (compared to the bulk one) is still uncertain,[14,16] the calculations were carried out for several values of $k_{hb} \equiv \varepsilon_s/\varepsilon_b$, in addition to several values of k_{LJ}. Different panels in Figure 1 correspond to different k_{hb} (0.8, 0.9, 1.0, and 1.1 from top to bottom) with $k_{LJ} = 0.603$, whereas different panels in Figure 2 correspond to different k_{LJ} (0.517, 0.603, 0.689, and 0.775 from top to bottom) with $k_{hb} = 1.0$.

As clear from Figures 1 and 2, the amplitude of the oscillations in the water density near the C_{60} fullerene decreases with increasing k_{hb}, but increases with increasing k_{LJ}. These oscillations are much more sensitive to k_{hb} than to k_{LJ}. For example, the height of the first oscillation peak increases by about 2% when k_{LJ} increases by 10%, while it increases by 10% when k_{hb} decreases by 10%. The oscillations of $\rho^{(1)}(r)$ are important[4,5] for the solvent-mediated repulsion of two C_{60} fullerenes. Each oscillation peak is associated with a hydration layer around the fullerene.

Figure 3 shows the fluid density profiles $\rho(q,z)$ (obtained from eq 6) between two C_{60} fullerenes for $q = 0$, i.e., along the axis z passing through the centers of both hydrophobes (one of the centers is at $z = 0$). Each figure panel corresponds to its own separation d_s (5η, 4η, 3.25η, and 2.5η).

As clear, approximation 6 in our combined DFT/PHB model predicts the behavior of $\rho(0,z)$ to be similar to that obtained via MD simulations.[4,5] As d_s decreases from ∞ to $d_s^b \approx 5\eta$, only bulk-like water is removed from between fullerenes, hence there is no solvent-mediated C_{60}−C_{60} interaction at $d_s \gtrsim d_s^b$. Decreasing d_s from d_s^b to $\approx 4\eta$ results in the gradual elimination of liquid water with density larger than the bulk one, so that the average density between fullerenes becomes smaller than the bulk. This corresponds to the elimination of the third hydration layer between fullerenes.

As d_s continues decreasing, the number of water molecules that are being displaced from between fullerenes alternately is either smaller than or larger than it would be if the water density between fullerenes were that of bulk liquid, depending on what part of the individual density profiles $\rho^{(1)}(r)$ are eliminated. This continues until the interfullerene space remains filled with the vapor-like water.

The water-mediated interaction between fullerenes is related to the structure of hydrating water in the interfullerene space. On the basis of MD simulations,[4,5] this interaction was concluded to be repulsive with oscillations depending on d_s. Although at any $d_s \lesssim d_s^b$ the potential of mean force (PMF) Φ of the solvent-induced interaction of two C_{60} fullerenes is positive (being 0 at $d_s \gtrsim d_s^b$), it is a nonmonotonic, oscillatory-decreasing function of d_s, i.e., the corresponding force alternates its sign with changing d_s, remaining mostly positive (which corresponds to repulsion).

DOI: 10.1021/acs.jpclett.5b00508
J. Phys. Chem. Lett. 2015, 6, 1761−1766

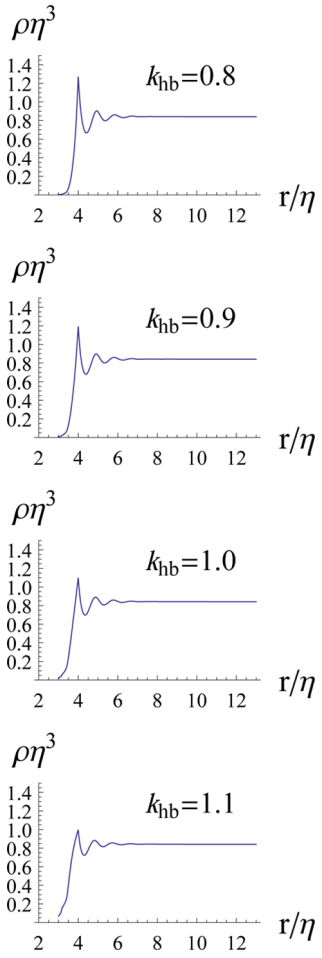

Figure 1. Fluid density profiles $\rho^{(1)} = \rho^{(1)}(r)$, in the vicinity of a single C_{60} fullerene shown in dimensionless units $\rho^{(1)}\eta^3$ versus r/η. Each figure panel corresponds to its own k_{hb} (=0.8, 0.9, 1.0, 1.1 from top to bottom), while k_{LJ} = 0.603 in all panels.

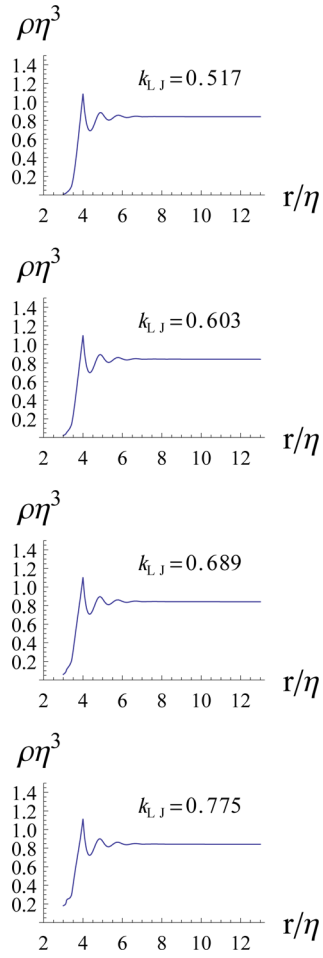

Figure 2. Fluid density profiles $\rho^{(1)} = \rho^{(1)}(r)$, in the vicinity of a single C_{60} fullerene shown as $\rho^{(1)}\eta^3$ vs r/η. Each figure panel corresponds to its own k_{LJ} (=0.517, 0.603, 0.689, 0.775 from top to bottom), while k_{hb} = 1.0 in all panels.

Using approximation (6), we calculated Φ for the interaction of two C_{60} fullerenes as a function of d_s. The numerical results are presented in Figure 4; the solid line is for k_{hb} = 0.9, dashed line for k_{hb} = 0.8, and dash-dotted line for k_{hb} = 1.1. The ratio k_{LJ} was set[5] to be equal to 0.603.

Our numerical result suggests that the hydrogen bonding ability of water plays a defining role in the unusual behavior of water-mediated interactions of C_{60} fullerenes. If the vicinal water−water hydrogen bonds were enhanced compared to bulk ones (e.g., k_{hb} = 1.1), the d_s-dependence of Φ would have a shape expected for conventional hydrophobes (monotonically increase with increasing d_s). This would correspond to an attractive solvent-mediated interaction between fullerenes.

However, if the vicinal water−water hydrogen bonds were weaker by 10% compared to bulk ones (e.g., k_{hb} = 0.9), the potential of mean force would be positive at the closest separation between the hydrophobes, d_s = 0, and the d_s-dependence of Φ would have an oscillatory shape similar to the one obtained by MD simulations;[4,5] remaining positive with increasing d_s, it reaches zero for $d_s \gtrsim d_s^b$. This oscillatory-repulsive character of Φ would become even more pronounced if the vicinal water−water hydrogen bonds were weaker by 20% compared to bulk ones.

As clear from Figure 4, for $k_{hb} < 1$ there are two metastable separations, $d_s \simeq 1.1\eta$ and $d_s \simeq 2\eta$, at which one or two hydration layers are well accommodated between fullerenes. At these separations the average water density therein corresponds to one that would be expected if all water, removed from between fullerenes upon decreasing d_s from ∞, were of bulk density.[5] Decreasing d_s from 2η to 1.1η, one of two hydration layers is gradually removed, which is thermodynamically unfavorable, thus giving rise to a local maximum in Φ at about 1.5η. At this separation the C_{60}−C_{60} solvent-mediated interaction changes from repulsive to attractive, and stays so until there remains a single water layer between fullerenes at $d_s \simeq 1.1\eta$, where Φ attains another local minimum. Decreasing d_s below 1.1η is accompanied by the removal of the last hydration layer from between fullerenes; this is thermodynamically unfavorable and the C_{60}−C_{60} solvent-mediated interaction is repulsive again until d_s becomes about 0.5η. At this separation, Φ reaches its global maximum, which corresponds[5] to the maximum in the number of molecules displaced from between fullerenes (compared to the number of molecules that would have been eliminated if water between fullerenes were bulk).

Thus, one can conclude that our numerical evaluations predict the solvent-induced interaction of two C_{60} fullerenes in water at 293 K to have an "oscillatory" repulsive character only when the vicinal water−water hydrogen bonds are weaker than bulk ones. Since such repulsion was previously observed in MD simulations,[5] our results suggest that (a) the hydrogen bonding

DOI: 10.1021/acs.jpclett.5b00508
J. Phys. Chem. Lett. 2015, 6, 1761−1766

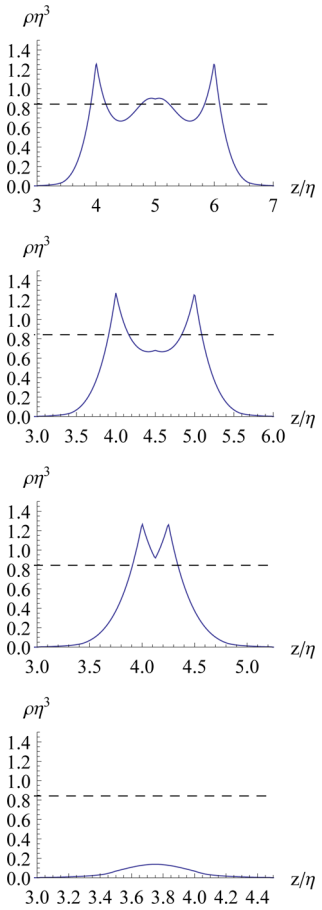

Figure 3. Fluid density profiles $\rho(q, z)$ between two C_{60} fullerenes at several separations d_s for $q = 0$, i.e., along the axis z passing through the centers of both hydrophobes. Each figure panel corresponds to its own separation d_s (=5η, 4η, 3.25η, 2.5η from top to bottom, respectively).

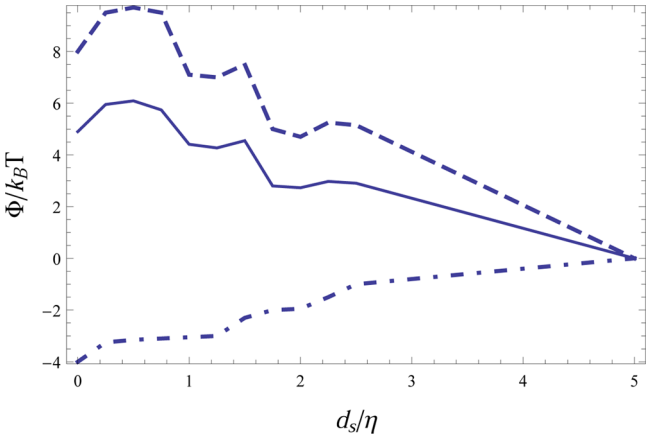

Figure 4. Potential of mean force Φ of the solvent-induced interaction of two C_{60} fullerenes as a function of separation d_s between them. The results are shown as Φ/k_BT versus d_s/η for $k_{hb} = 0.8$ (dashed curve), $k_{hb} = 0.9$ (solid curve), and $k_{hb} = 1.1$ (dash-dotted curve); all data are for $k_{LJ} = 0.603$.

ability of water plays a defining role in the solvent-mediated C_{60}−C_{60} interaction and (b) the energetic alteration of water−water hydrogen bonds near a C_{60} fullerene consists of their weakening.

That the weakening of water−water hydrogen bonds near fullerenes enhances the repulsive and oscillatory character of their solvent-mediated interaction is consistent with the energy-dominated nature of C_{60}−C_{60} repulsion.[4,5] Indeed, the weakening of vicinal hydrogen bonds results in larger water density oscillations around a single fullerene. Additionally, weaker and fewer hydrogen bonds per water molecule in the fullerene vicinity mean weaker and fewer constraints on vicinal water molecules compared to bulk ones, which would lead to a decrease in the system entropy upon displacing vicinal water molecules from the interfullerene space into the bulk. Both of these effects contribute to the enhancement of the solvent-mediated oscillatory repulsion of two fullerenes.

The macroscopic solution of C_{60} fullerenes in water is a colloidal system where the fullerenes exist as clusters. The stability of C_{60} colloids and size of C_{60} clusters are determined[14,26] by the adsorption of HO^- ions on C_{60} surface. The interactions between such aggregates are more difficult to model than the interaction between single fullerenes. The latter interaction, whereof the solvent-mediated component is considered in the foregoing, does govern the initial stages of C_{60} aggregation in water.

AUTHOR INFORMATION

Corresponding Authors

*E-mail: idjikaev@buffalo.edu.
*E-mail: feaeliru@buffalo.edu.

Notes

The authors declare no competing financial interest.

REFERENCES

(1) Kroto, H. W.; Heath, J. R.; O'Brien, S. C.; Curl, R. F.; Smalley, R. E. C_{60}: Buckminsterfullerene. *Nature* **1985**, *318* (6042), 162−163.
(2) Taylor, R. *The Chemistry of Fullerenes*; World Scientific: Singapore, 1995.
(3) Sheka, E. *Fullerenes: Nanochemistry, Nanomagnetism, Nanomedicine, Nanophotonics*. CRC Press: Boca Raton, FL, 2011.
(4) Li, L.; Bedrov, D.; Smith, G. D. Repulsive Solvent-Induced Interaction between C_{60} Fullerenes in Water. *Phys. Rev. E* **2005**, *71*, 011502.
(5) Li, L.; Bedrov, D.; Smith, G. D. A Molecular-Dynamics Simulations Study of Solvent-Induced Repulsion between C_{60} Fullerenes in Water. *J. Chem. Phys.* **2005**, *123*, 204504.
(6) Weiss, D. R.; Raschke, T. M.; Levitt, M. How Buckminsterfullerenes Affect Surrounding Water Structure. *J. Phys. Chem. B* **2008**, *112*, 2981−90.
(7) Friedman, S. H.; Decamp, D. L.; Sijbesma, R. P.; Srdanov, G.; Wudl, F.; Kenyon, G. L. Inhibition of the HIV-1 Protease by Fullerene Derivatives - Model-building Studies and Experimental Verification. *J. Am. Chem. Soc.* **1993**, *115*, 6506−09.
(8) Tokuyama, H.; Yamago, S.; Nakamura, E.; Shiraki, T.; Sugiura, Y. Photoinduced Biochemical Activity of Fullerene Carboxylic-Acid. *J. Am. Chem. Soc.* **1993**, *115*, 7918−19.
(9) Soda, K. Structural and Thermodynamic Aspects of the Hydrophobic Effect. *Adv. Biophys.* **1993**, *29*, 1−54.
(10) Chandler, D. Interfaces and the Driving Force of Hydrophobic Assembly. *Nature* **2005**, *437*, 640−647.
(11) Berne, B. J.; Weeks, J. D.; Zhou, R. Dewetting and Hydrophobic Interaction in Physical and Biological Systems. *Annu. Rev. Phys. Chem.* **2009**, *60*, 85−103.
(12) Zangi, R. Driving Force for Hydrophobic Interaction at Different Length Scales. *J. Phys. Chem. B* **2011**, *115*, 2303−11.
(13) Ma, X.; Wigington, B.; Bouchard, D. Fullerene C_{60}: Surface Energy and Interfacial Interactions in Aqueous Systems. *Langmuir* **2010**, *26*, 11886−11893.

DOI: 10.1021/acs.jpclett.5b00508
J. Phys. Chem. Lett. 2015, 6, 1761−1766

(14) Mchedlov-Petrossyan, N. O. Fullerenes in Liquid Media: An Unsettling Intrusion into the Solution Chemistry. *Chem. Rev.* **2013**, *113*, 5149−5193.
(15) Djikaev, Y. S.; Ruckenstein, E. The Variation of the Number of Hydrogen Bonds per Water Molecule in the Vicinity of a Hydrophobic Surface and its Effect on Hydrophobic Interactions. *Curr. Opin. Colloid Interface Sci.* **2011**, *16*, 272−284.
(16) Ruckenstein, E.; Djikaev, Y. S. Effect of Hydrogen Bonding between Water Molecules on Their Density Distribution near a Hydrophobic Surface. *J. Phys. Chem. Lett.* **2011**, *2*, 1382−1386.
(17) Djikaev, Y. S.; Ruckenstein, E. Effect of Water−Water Hydrogen Bonding on the Hydrophobic Hydration of Large-Scale Particles and its Temperature Dependence. *J. Phys. Chem. B* **2012**, *116*, 2820−2830.
(18) Djikaev, Y. S.; Ruckenstein, E. Probabilistic Approach to the Length-Scale Dependence of the Effect of Water Hydrogen Bonding on Hydrophobic Hydration. *J. Phys. Chem. B* **2013**, *117*, 7015−7025.
(19) Djikaev, Y. S.; Ruckenstein, E. The Solvent-Induced Interaction of Spherical Solutes in Associated and non-Associated Liquids. *J. Chem. Phys.* **2014**, *141*, 034705.
(20) Evans, R. Density Functional in the Theory of Nonuniform Fluids. In *Fundamentals of Inhomogeneous Fluids*; Henderson, D., Ed.; Marcel Dekker: New York, 1992.
(21) Hill, T. L. *Statistical Mechanics: Principles and Selected Applications*. Dover: New York, 1987.
(22) Tarazona, P. Free-Energy Density Functional for Hard Spheres. *Phys. Rev. A* **1995**, *31*, 2672−2679; **1995**, *32*, 3140 (erratum).
(23) Tarazona, P.; Marconi, U. M. B.; Evans, R. Phase Equilibria of Fluid Interfaces and Confined Fluids. Non-local versus Local Density Functionals. *Mol. Phys.* **1987**, *60*, 573−579.
(24) Carnahan, N. F.; Starling, K. E. Equation of State for Nonattracting Rigid Spheres. *J. Chem. Phys.* **1969**, *51*, 635−636.
(25) Weeks, J. D.; Chandler, D.; Anderson, H. C. Role of Repulsive Forces in Determining Equilibrium Structure of Simple Liquids. *J. Chem. Phys.* **1971**, *54*, 5237−5247.
(26) Bannerjee, S. J. Molecular Dynamics Study of Self-Agglomeration of Charged Fullerenes in Sovlents. *J. Chem. Phys.* **2013**, *138*, 044318.

DOI: 10.1021/acs.jpclett.5b00508
J. Phys. Chem. Lett. 2015, 6, 1761−1766